Part V

Icy Dwarf Planets and TNOs

Icy Bodies of the Solar System
Proceedings IAU Symposium No. 263, 2009
J.A. Fernández, D. Lazzaro, D. Prialnik & R. Schulz, eds.

doi:10.1017/S1743921310001717

Physical and dynamical characteristics of icy "dwarf planets" (plutoids)

Gonzalo Tancredi[1,2]

[1]Departamento Astronomía, Facultad de Ciencias, Montevideo, Uruguay
email: gonzalo@fisica.edu.uy

[2]Observatorio Astronómico Los Molinos, Ministerio de Educación y Cultura, Uruguay

Abstract. The geophysical and dynamical criteria introduced in the "Definition of a Planet in the Solar System" adopted by the International Astronomical Union are reviewed. The classification scheme approved by the IAU reflects dynamical and geophysical differences among planets, "dwarf planets" and "small Solar System bodies". We present, in the form of a decision tree, the set of questions to be considered in order to classify an object as an icy "dwarf planet" (a plutoid). We find that there are 15 very probable plutoids; plus possibly 9 more, which require a reliable estimate of their sizes. Finally, the most relevant physical and dynamical characteristics of the set of icy "dwarf planets" have been reviewed; e.g. the albedo, the lightcurve amplitude, the location in the different dynamical populations, the size distributions, and the discovery rate.

Keywords. solar system: general, "dwarf planets", plutoids, TNOs, Kuiper Belt

1. Introduction

In 2006 the XXVIth General Assembly of the International Astronomical Union adopted the Resolution 5: "Definition of a Planet in the Solar System". In this resolution 3 categories of objects orbiting around the Sun were distinguished: planets, "dwarf planets" and "small Solar System bodies"†.

There was also a Resolution 6 which established that "Pluto ... is recognized as the prototype of a new category of Trans-Neptunian Objects" and "an IAU process will be established to select a name for this category". On June, 2008, the Executive Committee of the IAU had decided on the term *plutoid* as a name for "dwarf planets" like Pluto.

Up to know 4 icy objects (plutoids) and one rocky object have been officially classified as "dwarf planets" by the IAU; i.e.: Eris, Pluto, Makemake, Haumea and Ceres. Nevertheless, there might exist many other objects which satisfy the criteria adopted in the Resolution 5 for "dwarf planets".

In the following sections, we review the scientific grounds of the resolution (Section 2), we present a list of potential icy "dwarf planets" (plutoids) (Section 3), and we discuss the main characteristics of this population of objects (Section 4).

We have adopted the following convention to define the transneptunian region: transneptunian objects (TNOs) have a semimajor axis greater than Neptune's one ($a > a_N$).

† The final text of the Resolution can be found in:
http://www.iau.org/static/resolutions/Resolution_GA26-5-6.pdf

2. The criteria to distinguish among the categories of Solar System objects

2.1. *The dynamical criterion*

According to the Resolution 5, the difference between planets and "dwarf planets" is that the former ones "have cleared the neighborhood around its orbit", while the second ones not. The problem of clearing the accretion zone were analyzed by Stern & Levison (2002) and Soter (2006).

The likelihood that in a timescale τ a small body would suffer an encounter with a planet that leads to a deflection of an angle θ is given by (Stern & Levison 2002):

$$\Lambda = \frac{\mu^2}{a_P^{3/2}} \left[\frac{\tau \sqrt{G M_\odot}(1+2\Gamma)}{2U^3 \pi^2 \sin(i) |U_x| \Gamma^2} \right] \tag{2.1}$$

where μ is the ratio between the planet's (M) and the solar mass ($M_\odot$); G is the gravitational constant; a_P is the semimajor axis of the planet (AU); i is the mutual inclination of the small body's orbit respect to the planet; U is the relative velocity of the small body and the planet in units of the of the planet's orbital velocity; U_x is the radial component of U; and $\Gamma \equiv \tan(\theta/2)$.

We assign values for the parameters that appear within the brackets in eq. (2.1) typical of a population of dynamically warm objects interacting with a planet. We assume a mean $e \approx \sin(i) \approx 0.1$, which corresponds to a Tisserand parameter $T \approx 2.98$ and $U = \sqrt{3-T} \approx 0.14$. U_x is calculated from the assumption of isotropical decomposition between the 3 components; i.e. $U_x = U/\sqrt{3}$. The clearing of the accretion zone would occur if the deflection angle is large, let's say $\theta \approx 1$; i.e. $\Gamma \approx 1/2$.

Since the adopted planet definition applies to objects in the Solar System, we consider the age of the Solar System as the relevant timescale for the clearing process; i.e. $\tau \approx 4.5 \times 10^9$ yr. Note that Stern & Levison (2002) and Soter (2006) use instead the age of the Universe for the relevant timescale.

According to the previous considerations, the condition for clearing the neighborhood around its orbit can be translated into the following condition for the mass:

$$\mu > \sqrt{\frac{a_P^{3/2}}{5 \times 10^{14}}} \tag{2.2}$$

In Fig. 1 we plot the masses of the planets and several massive asteroids and TNOs as a function of the semimajor axis in logarithmic scale. A couple of vertical dashed lines are included in the plots that corresponds to the possible inner and outer limits of the so-called "snow line", the heliocentric distance where the water condensates. A thick full-line is also drawn which corresponds to the condition of eq. (2.2). There is a huge gap of 3-4 order of magnitude in mass between planets and "dwarf planets" in the inner or outer region of the Solar System. The condition for clearing the neighborhood stated above clearly separates the two type of objects.

2.2. *The geophysical criterion*

A geophysical criterion separates planets and "dwarf planets" from the group of "small Solar System bodies". The former ones "have sufficient mass for its self-gravity to overcome rigid body forces so that it assumes a hydrostatic equilibrium (nearly round) shape". The geophysical criterion introduced in the definition distinguishes between objects that had suffered (or not) important internal transformations due to the action of the self-gravitation. It separates between two extreme cases: objects that are just an

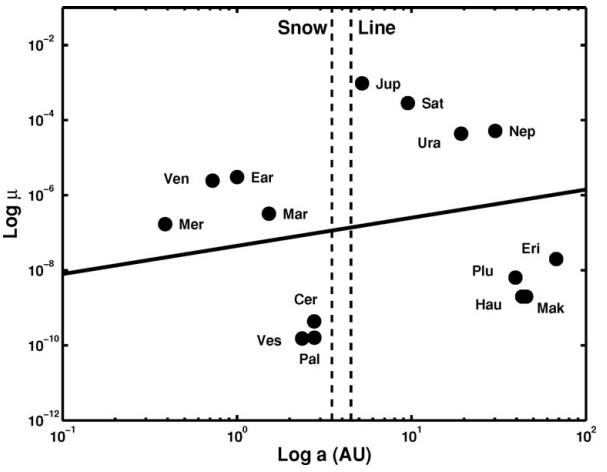

Figure 1. The ratio (μ) between the planet's and the solar mass versus the semimajor axis of the planet in AU (a) in logarithmic scale for the planets and several massive asteroids and TNOs. See the text for the explanation of the additional lines.

agglomeration of planetesimals with little mutual cohesion (the "small Solar System bodies"); and objects where the material has been largely metamorphosed due to the high pressure and temperatures produced under the weight of the outer layers (planets and "dwarf planets"). The former ones adopt an irregular shape, while the later ones tend to acquire a figure in hydrostatic equilibrium. Tancredi & Favre (2008) (hereafter Paper I) has revised the information about Solar System objects in hydrostatic equilibrium either from the theoretical and the observational perspective.

The definition takes into account two concepts that we discuss below: i) the figures of equilibrium and ii) the overcome of rigid body forces by the self-gravity.

For an strengthless isolated object in rotation, the equilibrium figures are a set of ellipsoidal shapes depending on the angular momentum. Chandrasekhar (1987) introduced two dimensionless parameter to characterize the problem: one associated with the angular momentum ($\Gamma = L/(GM^3R)^{1/2}$), where L is the angular momentum, G is the gravitational constant, M the mass and R the radius; and the other one is associated with the angular velocity ($\Omega = \omega^2/(\pi G\rho)$), where ω is the angular velocity and ρ is the density. A non-rotating body acquires a spherical shape, while a body with a low angular momentum acquires the figure of an oblate ellipsoid (a MacLaurin spheroid two equal axes larger than the third axis). For higher angular momentum ($\Gamma > 0.303$), the body acquires a triaxial ellipsoidal figure (a Jacobi ellipsoid), up to a critical value of $\Gamma = 0.39$ where the body becomes unstable against further increase of the angular momentum (see Fig. 1a in Paper I). In the range $0.303 < \Gamma < 0.39$, although the angular momentum increases, the angular velocity is being reduced while the figure becomes more elongated. The ratios between the axis for the Jacobi ellipsoids go from $b/a = 1$ and $c/a = 0.583$ at the transition between MacLaurin to Jacobi ellipsoids, to $b/a = 0.432$ and $c/a = 0.345$ at the edge of instability. In the same range the dimensionless angular velocity is being reduced from $\Omega < 0.374$ to 0.284 (see Fig. 1b in Paper I). Therefore, for bodies with densities over 1 gcm^{-3}, the full rotational period is constrained to values less than 7.15h.

Assuming a strengthless isolated object, we then have a given relation between the rotational period, the shape (represented by the axis ratios of an ellipsoid) and the density for figures in hydrostatic equilibrium.

Different criteria have been used in the literature to estimate the condition when a self-gravitating body overcomes the material strength. All the criteria reduce to the following expression that relates the critical diameter (D) for a self-gravitating body to overcome the material strength, the density (ρ) and the material strength (S) (Paper I):

$$D\rho/2 = \alpha\sqrt{\frac{3}{2\pi G}}\sqrt{S} \tag{2.3}$$

where α is a parameter that depends on the chosen criteria, but it has typical values in the range $1 < \alpha < 5^{1/2}$ (Note that in eq. 2.3 we correct a typo that appeared in eq. 1 of Paper I; a division by 2 of the diameter was missing in that eq.; nevertheless the computations based on this eq. and the plots were correct). The material strength depends on the constituents and the temperature. Typical values for mixtures of ice and soil are in the range of a few tens to a few hundreds MPa (Petrovic 2003).

From the observational perspective it is possible to put some constraints from the analysis of the shapes of the icy bodies visited by spacecrafts; e.g. the icy satellites of the outer planets. In Paper I it was found that the Saturnian satellite Mimas and the Neptunian satellite Proteus are among the smallest objects with a figure close to equilibrium. It was noticed a possible dependence of the critical diameter with the temperature, as it was expected. They concluded that in the TNO region the transition to an equilibrium figure should occur at a value of $D\rho \sim 600$ km gcm^{-3}. Assuming a value of $\rho = 1.3$ gcm^{-3} (typical of the Uranian and Neptunian satellites of this size), the critical size for TNOs is $D \sim 450$ km. This value is in correspondence to the theoretical critical limit presented above for a low-strength material of $S \sim 1 - 10$ MPa and $\rho \sim 1 - 2$ gcm^{-3}.

Therefore, we will use the value $D \sim 450$ km as the limit between "dwarf planets" and "small Solar System bodies" in the transneptunian region.

3. The list of icy "dwarf planets"

Unless the case of Pluto and Eris, there are not direct estimates of the size of the TNOs. A model dependent estimate of the size comes from measurements of thermal emission using IR space telescopes. Using the Spitzer Space Telescope Stansberry *et al.* (2008) obtain size estimates of a large fraction of the largest TNOs. Combined with accurate determinations of the absolute magnitude in V (H), it is possible to compute the geometrical albedo (p_V). In Fig. 2 we plot p_V against the diameter (D in km) from the data collected by Stansberry *et al.* (2008).

Finally, a rough idea of the size can be obtained from the total absolute magnitude and an assumed value for the geometrical albedo. There is a wide range of albedo estimates for TNOs, from values of $0.6 - 0.8$ for the largest objects down to values of 0.03 (see Fig. 2). Assuming the constraint $p_V \leqslant 1$, objects with an absolute magnitude brighter than $H < 2.4$ are certainly larger than 450 km. For the TNOs without size estimates, we assume a conservative value $p_V = 0.1$ to left behind as less dwarf candidates as possible. A diameter of 450 km would correspond to $H < 4.9$ for this given albedo.

From the list of TNOs listed by the Minor Planet Center by July 22, 2009 (†) and the list of objects observed by Stansberry *et al.* (2008), we extract 46 objects with an estimated size larger than 450 km. This list is an updated version of the one presented in Paper I. This preliminary list of icy dwarf candidates is presented in Table 1. The objects are listed in increasing order of absolute magnitude H.

† The latest lists of TNOs and Scattered Disk Objects is given in: http://www.cfa.harvard.edu/iau/lists/MPLists.html

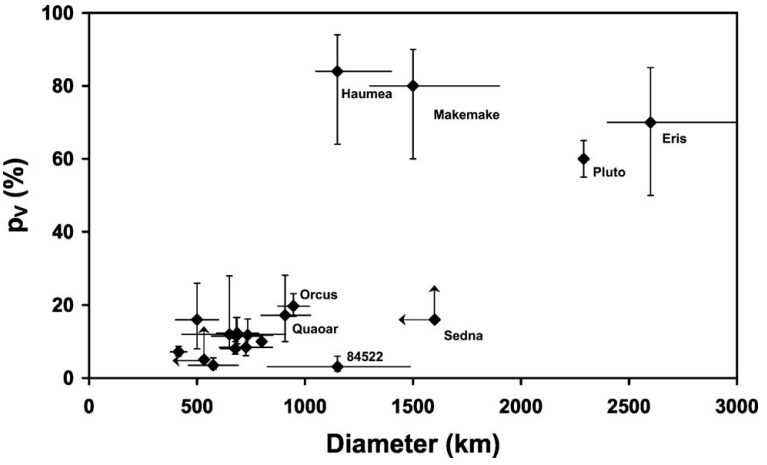

Figure 2. Plot of the geometrical albedo (p_V) against the diameter (D in km) from the data collected by Stansberry *et al.* (2008). We include the error bars as stated by the authors.

In order to finally classify these objects as "dwarf planets", we have to get some information about their shapes. In Paper I, it was proposed to analyze the rotational lightcurve, i.e. the variation of the observed brightness as a function of the rotational phase angle. The brightness is proportional to the projected shape in the sky and the surface albedo. A sphere or MacLaurin spheroid with uniform albedo distribution produces a flat lightcurve; while a Jacobi ellipsoid produces a lightcurve with two identical maximum peaks. The existence of albedo spots could introduce weird patterns, but the vast experience in asteroidal lightcurves has shown that the albedo contribution is generally less important than the shape (Magnusson 1991).

The viewing geometry also affect the shape of the lightcurve of an ellipsoidal figure. The maximum amplitude is obtained when the observer is in the plane of the object's equator; and it is reduced to zero if the object is pole on. For the following analysis, since we do not have any information of the viewing geometry, we will assume that the observed amplitudes correspond to the maximum amplitude for the object. Unfortunately, this situation can not change in the near future because, due to the slow movement of the TNOs, the viewing geometry may take decades to show a significant variation.

In the case that the lightcurve amplitude is small ($\Delta m < 0.15$), we can considered the object as a small departure from a sphere or MacLaurin spheroid with small albedo spots. But if the amplitude is larger than the previous value, we have to analyze whether the observed lightcurve is compatible with the lightcurve produced by a Jacobi ellipsoid of a plausible density range.

For an ellipsoidal figure, the square of the projected shape in the sky as a function of time can be described as a Fourier series of order 2 with a null term of order 1 (see Barucci *et al.* (1989)) and eq. 2 in Paper I). We make the assumption that the brightness is directly proportional to the projected shape. Therefore, if we develop the square of the brightness in a Fourier series up to order two, the ratio between the quadratic sums of the coefficients of order one and two (defined as the β parameter) is an indicator of the closeness to an ellipsoidal shape. Values of $\beta \sim 0$ would correspond to a perfect ellipsoid.

After modeling synthetic lightcurves, it was found that important departures from an ellipsoidal shape comparable to the ones observed in the irregular satellites can be detected if the value of $\beta \geqslant 0.25$ (see Paper I). Therefore, lightcurves with $\beta \geqslant 0.25$ can be discarded as produced by a smooth ellipsoid. If $\beta < 0.25$, the shape deduced from the

Table 1. List of icy "dwarf planets" candidates.

Number	Name	Provisional Designation	Abs. Mag. H_V	Diameter (km)	Dwarf	Case
136199	Eris	2003 UB313	-1.1	2600	Yes	I
134340	Pluto		-0.7	2390	Yes	I
136472	Makemake	2005 FY9	0	1500	Yes	II
136108	Haumea	2003 EL61	0.5	1150	Yes	III
90377	Sedna	2003 VB12	1.8	1600	Yes	II
		2007 OR10	1.9	# 1752		
90482	Orcus	2004 DW	2.5	946	Yes	II
50000	Quaoar	2002 LM60	2.6	908	Yes	II
		2005 QU182	3.1	# 1008		
202421		2005 UQ513	3.4	878		
55636		2002 TX300	3.49	800	Yes	II
174567		2003 MW12	3.6	# 801	Yes?	II
		2007 UK126	3.6	# 801		
55565		2002 AW197	3.61	735	Yes	II
		2003 AZ84	3.71	686	Yes	II
55637		2002 UX25	3.8	681	???	V
		2006 QH181	3.8	# 730		
28978	Ixion	2001 KX76	3.84	650	Yes	II
145452		2005 RN43	3.9	# 697	Yes?	II
20000	Varuna	2000 WR106	3.99	500	Yes	III
		2002 MS4	4	726		
145453		2005 RR43	4	# 666	Yes?	II
		2004 XA192	4	# 666		
84522		2002 TC302	4.1	1150		
120178		2003 OP32	4.1	# 636	Yes?	III
90568		2004 GV9	4.2	677	Yes	II
84922		2003 VS2	4.2	# 607	No	IV
42301		2001 UR163	4.2	# 607	Yes?	II
120347		2004 SB60	4.2	# 607	Yes?	II
		2003 UZ413	4.3	# 580		
119951		2002 KX14	4.4	# 554		
145451		2005 RM43	4.4	# 554	Yes?	II
		2004 NT33	4.4	# 554		
120348		2004 TY364	4.5	# 529	No	IV
		2004 XR190	4.5	# 529		
144897		2004 UX10	4.5	# 529	Yes?	II
-19308		1996 TO66	4.5	# 529		
		2004 PR107	4.6	# 505		
26375		1999 DE9	4.7	# 482	Yes?	II
145480		2005 TB190	4.7	# 482		
		2007 JH43	4.7	# 482		
		2003 QX113	4.7	# 482		
175113		2004 PF115	4.7	# 482		
24835		1995 SM55	4.8	# 461	No	IV
38628	Huya	2000 EB173	5.23	533	Yes	II
15874		1996 TL66	5.46	575	Yes	II

lightcurve can be approximated to an ellipsoid; but, is it an ellipsoid of the Jacobi-family? The Jacobi ellipsoids have a given set of relations between the axis ratios, the rotational period and the density, as it was stated in Subsection 2.2 (see Fig. 1b in Paper I). From the lightcurve, we obtain the rotational period and a possible range of ratios of the two major axis (b/a), depending on the aspect angle at the time of the observation (the angle between the rotation axes and the visual). Based in the equations for the Jacobi ellipsoids

(Chandrasekhar 1987, and Paper I), a range of densities compatible with the data can be found. Since, all the icy satellites with equilibrium-shape bodies and the large TNOs have densities $\rho > 1$ gcm^{-3}, we accept candidates for an icy "dwarf planet" with a Jacobi shape, if there are estimates of the density based in the previous calculations with values larger than 1 gcm^{-3}.

The previous set of criteria to qualify a candidate as an icy "dwarf planet" was presented in detail in Paper I, but here we have compiled them in the decision tree presented in Fig. 3.

We apply this decision tree to the list of "dwarf planet" candidates listed in Table 1. A column is added to answer the question: is the object a "dwarf planet"? The following answers are considered to this question:

- *Yes* - accepted as a "dwarf planet"
- *Yes?* - possibly acceptable case, those are objects that show very small amplitudes, but we do not have enough information to support the size estimate
- *No* - rejected as a "dwarf planet"
- *???* - the observational evidence is conflicting: the object seems to be larger than 450 km based on the IR data, but there are important differences between the lightcurve data among different observers.
- blank space - for objects without a lightcurve or any other kind of information to decide whether they can be considered as "dwarf planets" or not.

In addition we include in Table 1 another column to list under which of the Cases presented in the decision tree the object is accepted or rejected.

The information compiled in Table 1 is presented in detail, as well as the photometric data on which we base our classification and the links to the corresponding references, in the webpage: *"Dwarf Planets" Headquarters: http://www.astronomia.edu.uy/dwarfplanet.*

4. Characteristics of icy "dwarf planets" (plutoids)

The individual characteristics of the very large TNOs has been revised by Brown (2008). He presented a detailed discussion of the physical properties of the first 5 object in Table 1. Each of these objects presents particular features that deserve a detailed analysis. For further reading on these individual cases, the reader should refer to Brown's chapter and to the large number of papers dealing with observational data of these objects that have appeared in the literature in the recent years.

Instead, we decided to analyze the collective properties of the several tens largest TNOs. In the following section we review the scant information available regarding the physical and dynamical properties of this set of objects.

4.1. *The physical characteristics*

In Fig. 2 we have already presented the most reliable estimates of the geometrical albedo (p_V) against the diameter (D in km) coming from the Spitzer observations collected by Stansberry *et al.* (2008). Two clear sets can be identified: *i*): very large TNOs with sizes over 1000 km and very high albedos ($p_V \sim 0.6 - 0.9$); *ii*): objects with low albedos ($p_V \lesssim 0.2$) and diameters less than 1000 km. There might be a couple of objects with sizes over 1000 km but low albedos (Sedna and 84522); but the estimates are very uncertain since they are based on observations with a $SNR < 5$. The difference between larger and smaller TNOs can be interpreted as the capacity of larger objects to retain an atmosphere with a seasonal evolution. The larger objects could have deposits of fresh and high albedo ices on their surfaces, while the smaller objects present a weathered and darker surface. A physical modeling of this process would be desirable.

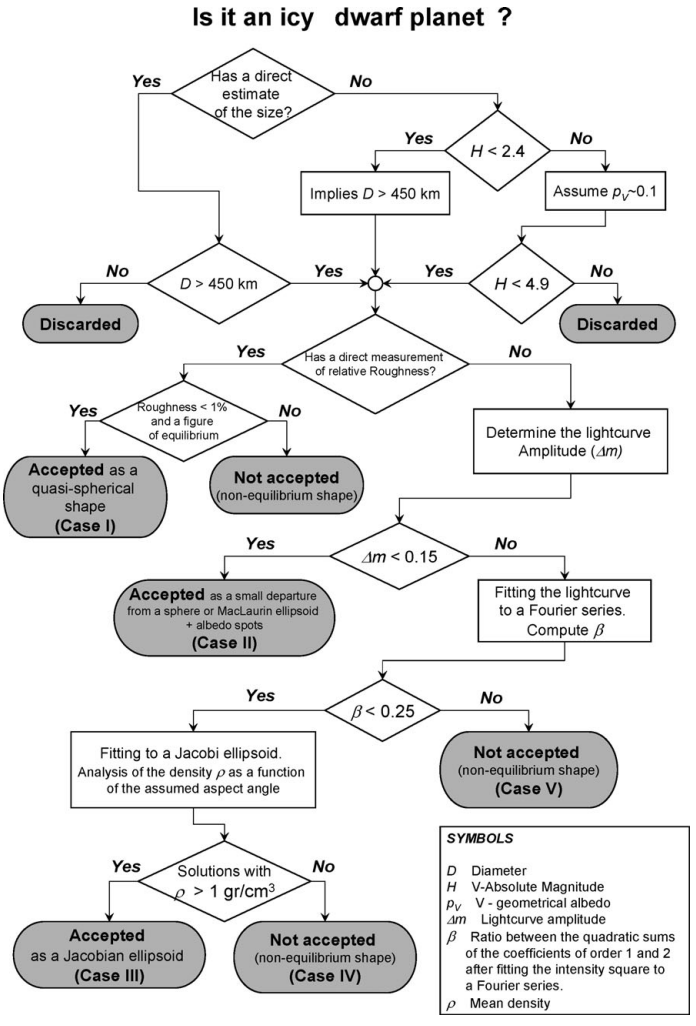

Figure 3. Decision tree to qualify a candidate as an icy "dwarf planet" (plutoid).

The results of a large observational campaign with photometric observations of several objects included in our list is being published by Thirouin *et al.* (2009). This data set constitutes the basis for a compilation of an extended database of light curve parameters that has appeared in the literature produced by Duffard *et al.* (2009). The authors obtain the mean rotational properties of the entire sample, determine the spin frequency distribution and search for correlations between different physical and orbital parameters (rotational period, peak-to-peak amplitude, semimajor axis, perihelion distance, aphelion distance, eccentricity, inclination). Among the conclusions presented by the authors we highlight the following ones: *i)* they found a correlation between the rotational period and the B-V color which might suggest that objects with shorter rotation periods may have suffered more collisions than objects with longer ones; *ii)* there is also a correlation between the amplitude and the absolute magnitude H which indicates that the smaller (and collisionally evolved) objects are more elongated than the bigger ones. Using their dataset, in Fig. 4a we show the later correlation between the amplitude and H. A vertical line at $H = 4.9$ is drawn to separate the "dwarf planet" candidates and the smaller objects.

The authors also conclude from the results of their model, that hydrostatic equilibrium is probably reached by almost all TNOs brighter than $H < 7$. In order to reassess this topic, we plot in Fig. 4b the single peak period vs the observed amplitude for the TNOs brighter than $H < 7$ in their dataset. The points can be divided in two groups: objects with low amplitudes and large periods, and objects with high-amplitudes and small periods. Three sets of objects are shown in the figure: *i)* full squares - objects with $H < 4.9$ not discarded as "dwarf planet" candidates; *ii)* empty squares - objects with $H < 4.9$ but discarded as "dwarf planet" candidates; and *iii)* empty diamonds - objects with $4.9 < H < 7$. We also draw a few lines that correspond to the relation between the period and the maximum amplitude of strengthless ellipsoidal figures of equilibrium with several densities (see Paper I for further details on how these lines are calculated). The lower curves correspond to the relation between the maximum lightcurve amplitude and half the period for Jacobi ellipsoids with densities $\rho = 0.5$, 1, 2 and 5 gcm^{-3}. The two upper horizontal lines correspond to a MacLaurin spheroid with density $\rho = 1$ and 2 gcm^{-3}, respectively.

Densities lower than 1 gcm^{-3} are required in order to be in hydrostatic equilibrium for most of the high amplitude objects ($\Delta m > 0.15$) with smaller sizes ($4.9 < H < 7$, empty diamonds in the plot). Even much lower densities are required in a few cases. Although we can not rule out that these smaller objects are in hydrostatic equilibrium, we point out that all the satellites of the outer planets larger than 100 km have densities higher than $\rho \gtrsim 1$ gcm^{-3}, with the exception of Hyperion†. In view of these evidences, we think that the conclusion of Duffard *et al.* (2009) that "hydrostatic equilibrium is probably reached by almost all TNOs brighter than $H < 7$ must deserve a more detailed analysis.

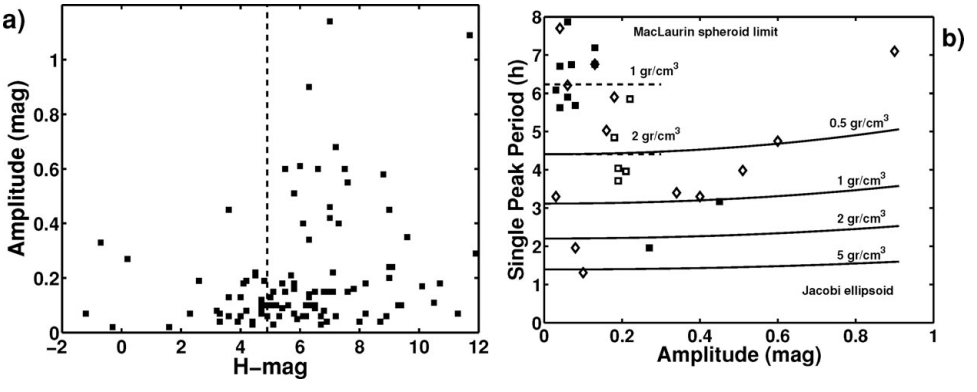

Figure 4. *a)* The lightcurve amplitude versus the absolute magnitude (H). The data is taken from Duffard *et al.* (2009). *b)* The amplitude versus the rotational period for the same data set. See the text for an explanation on the different symbols and the lines drawn in the plot.

4.2. *The dynamical characteristics*

In Fig. 5 a and b we plot the inclination (i) and eccentricity (e) versus the semimajor axis (a) for objects outside Uranus orbit. The objects are represented by a small black dot and a gray-shaded circle proportional to its diameter. The diameter scale is represented by an empty circle of 1000 km.

We note that most of the objects in Fig. 5 with noticeable diameters (typically larger than a few hundred km) are located in the so-called hot population of the transneptunian

† See e.g. the compilation of Physical Parameters of the Planetary Satellites at the Jet Propulsion Laboratory website and the references therein: http://ssd.jpl.nasa.gov/?sat_phys_par.

region, the region of high-i and high-e, e.g. $i \gtrsim 15\,\mathrm{deg}$ and $e \gtrsim 0.1$. This result is reflected in the distribution of these parameters; while for the complete sample of objects with semimajor axis greater than Neptune's one, the mean inclination is $\overline{i}_{all} = 9.8\,\mathrm{deg}$, for the restricted sample of "dwarf planet" candidates is $\overline{i}_{dwarf} = 20.6\,\mathrm{deg}$. For the eccentricity the corresponding values for the two samples are $\overline{e}_{all} = 0.18$ and $\overline{e}_{dwarf} = 0.22$, respectively. The Kolmogorov-Smirnov test applied to both the distribution of i and e shows that the hypothesis that the two samples come from the same underlying one-dimensional probability is rejected at the 90% confidence level.

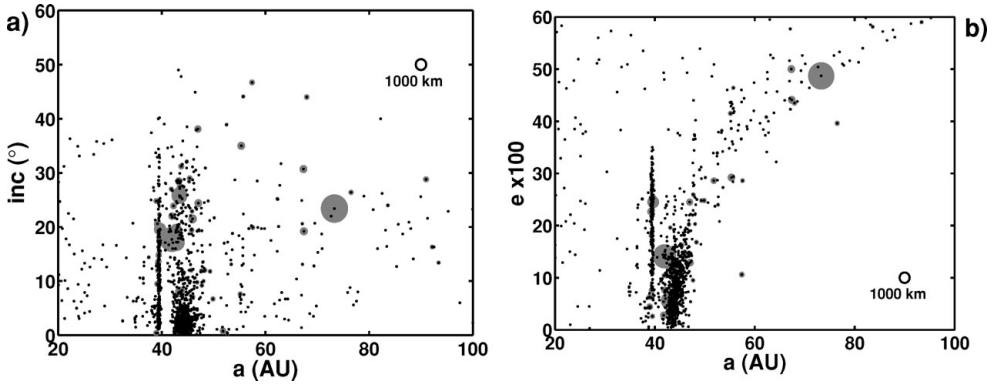

Figure 5. Plots of the dynamical parameters of TNOs. *a)* Inclination versus semimajor axis. *b)* Eccentricity versus semimajor axis.

The size segregation between large objects in the hot population and almost lack of large ones in the cold population has not been successfully explained by any of the prevailing cosmogonical models, like the Nice model (see e.g. Gomes 2003, 2009). It is an open problem yet to be solved.

4.3. *The size distribution*

Considering the accretional and collisional processes experienced by the transneptunian objects, it is expected that the cumulative size distribution should follow a power-law of an exponent close to 3. As mentioned above a proxy of the size is the absolute magnitude, but the relation between these two parameters depends on the geometrical albedo. For a fixed value of the albedo, a power-law cumulative size distribution of exponent α should correspond to a cumulative absolute magnitude distribution with a slope $s = \alpha/5$.

The size distribution of the TNOs has been revised by Petit *et al.* (2008). Most of the estimates of the size distribution relies on the computation of the luminosity function (LF), i.e. the cumulative number of TNOs brighter than a given apparent magnitude. Converting the LF into a size distribution involves the modeling of the dynamical and physical surface properties of the TNOs. Petit *et al.* (2008) compiled the results of several papers that address this question. A wide range of LF slopes has appeared in the literature from 0.3 to 0.9; which it can be transformed into an exponent of the cumulative size distribution in the range $\alpha \sim 3 - 4$ for bodies larger than a few tens of kilometers (Note that we use the cumulative exponent while Petit *et al.* (2008) use the differential one).

The cumulative absolute magnitude distribution is presented in Fig. 6a. An overabundance of bright objects over the dashed linear fit is observed, as it has already been noted by e.g. Brown (2008). A similar overabundance of large objects should appear in the size distribution if it is computed from the previous magnitude distribution and assuming a fixed albedo, as it is usual. Nevertheless, nowadays there is a large sample of TNOs with

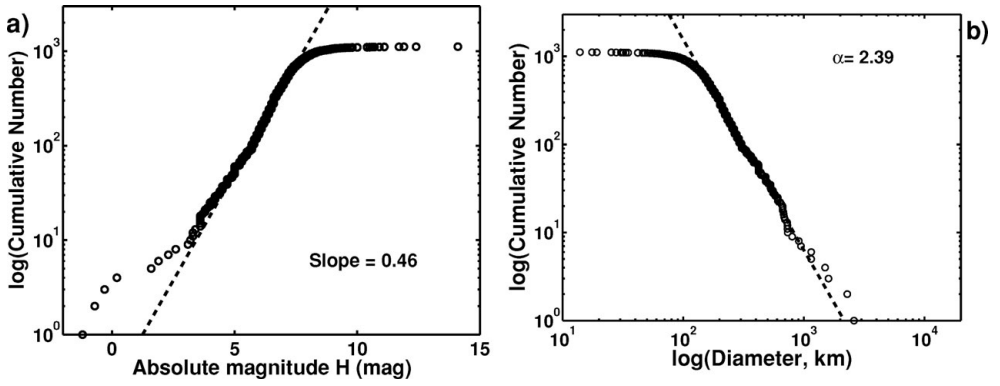

Figure 6. *a)* Cumulative distribution of absolute magnitude with the Number in logarithmic scale. *b)* Cumulative size distribution of in log-log scale.

reliable size estimates (Stansberry *et al.* 2008) that can be taken into account. Combining the diameters listed in Stansberry *et al.* (2008) dataset with the estimates derived from the absolute magnitude and a common albedo $p_V = 0.1$, we obtain the size distribution of the observed sample of TNOs presented in Fig. 6b. The overabundance of large TNOs has disappeared due to the correlation between sizes and albedo noted in Fig. 2. A good fit to a power-law is obtained for $D > 150$ km with an exponent $\alpha = 2.39$. Our dataset has not been corrected for observational biases, and this could partially explain the differences with previous estimates of the cumulative exponent. A new analysis with a proper correction of the observational biases is left for a future work; nevertheless we have shown that a better treatment of the observational data, which includes different sources of information, could improve the quality of the adjustment.

4.4. *How many plutoids are still missing?*

After the discovery of the third member of the transneptunian region in 1992 (1992QW1), the discovery rate had suffered a continuous increase up to the early 2000's (Fig. 7a). In the second half of this decade the discovery rate has decreased considerably, due to the fact that the number of wide-area surveys of TNOs has been drastically reduced (see Petit *et al.* (2008) for a list of the most relevant surveys). Until July 2009 there were discovered 904 TNOs brighter than $H > 8.1$ (larger than 100 km for $p_V = 0.1$). But Petit *et al.* (2008) estimated that there should be $\sim 10^4$ larger than this size; therefore, we are far to reach completeness.

A similar conclusion can be drawn from Fig. 7b where we plot the absolute magnitude H versus the discovery year. A clustering of the discoveries in the years 1999 to 2006 is observed. In Fig. 7b we also draw a horizontal dashed-line at $H = 4.9$, the limiting magnitude we have used for "dwarf planet" candidates. Almost all the "dwarf planet" candidates were discovered in the period 1999-2006; in particular 8 out of 10 of the absolute brightest ones were discovered by the survey lead by Brown (2008) which used the 48-inch Palomar Schmidt telescope (one object among this 8 was independently discovered by Aceituno *et al.* 2005).

If we assume that the size distribution with an exponent in the range $\alpha \sim 3 - 4$ extends down to objects of several hundred km, there should be between a few tens to a less than a couple of hundreds "dwarf planets" with $H < 4.9$ and sizes larger than 450 km. Therefore, we may be half the way to reach completeness for the large sample of TNOs.

The Palomar survey for large TNOs covered 20.000 deg^2 north of -30 deg declination (Brown 2008). Unfortunately there is no assessment of the efficiency of this survey.

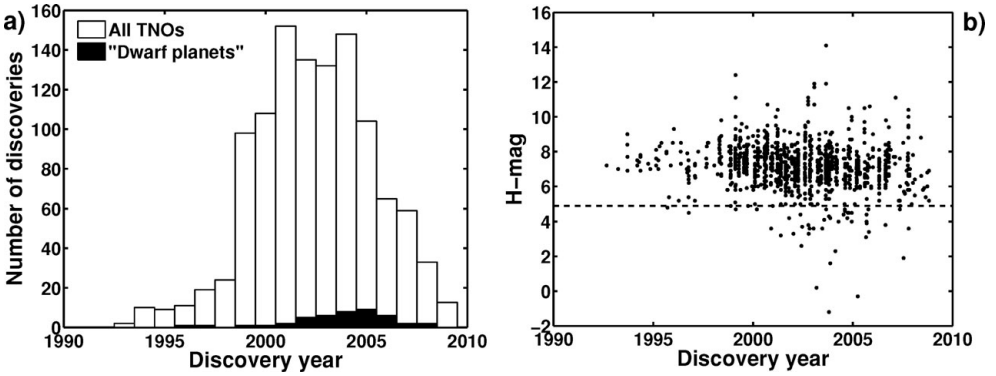

Figure 7. *a)* The number of discoveries per year as a function of the discovery year. *b)* The absolute magnitude (H) versus the discovery year. An horizontal dashed-line at $H = 4.9$ is drawn.

Assuming a 100% for the very bright objects $H < 1$ (the limit for the 4 IAU's "official" plutoids), there should be 3-4 similar objects yet to be discovered; one of them should be close to the galactic plane, since this region was not covered by the Palomar survey; and ~ 3 should be in the region south of -30 deg declination.

5. Conclusions

We have reviewed the scientific grounds of the "Definition of a Planet in the Solar System" adopted by the XXVI General Assembly of the IAU. The two criteria used in the definition have been discussed: *i)* the dynamical criterion that separates planet and "dwarf planets"; and *ii)* the geophysical criterion that separates "dwarf planets" and the "small Solar System bodies". The classification scheme approved by the IAU reflects important dynamical and geophysical differences among the three set of objects in the Solar System.

We update the list of "dwarf planet" candidates that was initially presented by Tancredi & Favre (2008). The set of criteria to decide whether a candidate has a figure in hydrostatic equilibrium, and therefore it can be considered as a "dwarf planet", is presented for clarity as a decision tree.

After applying this decision tree to the list of candidates, we find that there are 15 very probable icy "dwarf planets" (plutoids), plus possibly 9 more, but we are lacking of reliable estimate of their sizes (they are listed in Table 1 with a *Yes?*). Three objects with preliminary estimated diameter larger than 450 km were discarded as "dwarf planets"; and one case where the observational evidence is conflicting. There are 18 objects with sizes possibly over the critical limit but they require further observations of the lightcurve and/or the size to consider them as "dwarf planets".

Finally, the most relevant physical and dynamical characteristics of the set of icy "dwarf planets" have been revised. We highlight the following conclusions:

(a) There is a remarkable difference between very large icy "dwarf planets" with high-albedos and smaller ones with low albedos. The difference can be interpreted as the capacity of larger objects to retain an atmosphere with a seasonal evolution, but a modeling of this process is encouraged.

(b) Objects with sizes estimates clearly over the limit of 450 km which present large amplitude lightcurves, have an elongated shape that is compatible with a Jacobi ellipsoids with densities $\rho > 1$ gcm^{-3} But, in the case of objects in the size range 100 to 450 km

with large amplitude lightcurves, densities much lower than 1 gcm^{-3} are required in order to be compatible with a Jacobi ellipsoid.

(*c*) There is a size segregation between large objects in the hot population and almost lack of large ones in the cold population that has not been successfully explained by any of the prevailing cosmogonical models.

(*d*) An overabundance of bright objects is observed in the cumulative absolute magnitude distribution; but this overabundance does not appear in the cumulative size distribution if the reliable sizes estimates based on IR data are included.

(*e*) There might be several tens up to more than a hundred objects larger than 450 km yet to be discovered. Among the very large ones ($H < 1$, the limit for the 4 IAU's "official" plutoids), there should be 3-4 similar objects yet missing.

To the end, we would like to raise the question: Should the IAU continue naming "dwarf planets"? In order to proceed cautiously, we suggest that the following objects could be included in the list of "official" "dwarf planets": (90377) Sedna, (90482) Orcus and (50000) Quaoar. These objects are clearly over the size limit of 450 km and the photometric observational evidence are in concordance with a figure in hydrostatic equilibrium.

References

Aceituno, J., Santos-Sanz, P., & Ortiz, J. L. 2005, *M.P.E.C.*, 2005-O36

Barucci, M. Capria, M., Harris, A., & Fulchignoni, M. 1989, *Icarus*, 78, 311

Brown, M. 2008, in: M. A. Barucci, H. Boehnhardt, D. P. Cruikshank & A. Morbidelli (eds.), *The Solar System Beyond Neptune* (University of Arizona Press, Tucson), p. 335

Chandrasekhar, R. 1987, *Ellipsoidal Figures of Equillibrium*, Dover Publications, New York

Duffard, R., Ortiz, J. L., Thirouin, A., Santos-Sanz, P., & Morales, N. 2009, *A&A*, 505, 1283

Gomes, R. S. 2003, *Icarus*, 161, 404

Gomes, R. S. 2003, *Celest. Mech. Dyn. Astr.*, 104, 39

Magnusson, P. 1991, *A&A*, 243, 512

Petit, J.-M., Kavelaars, J. J., Gladman, B., & Loredo, T. 2008, in: M. A. Barucci, H. Boehnhardt, D. P. Cruikshank & A. Morbidelli (eds.), *The Solar System Beyond Neptune* (University of Arizona Press, Tucson), p. 71

Petrovic, J. 2003, *J. Materials Science*, 38, 1

Soter, S. 2006, *AJ*, 132, 2513

Stansberry, J. A., Grundy, W. G., Brown, M., Cruikshank, D. P., Spencer, J., Trilling, D., & Margot, J. L. 2008, in: M. A. Barucci, H. Boehnhardt, D. P. Cruikshank & A. Morbidelli (eds.), *The Solar System Beyond Neptune* (University of Arizona Press, Tucson), p. 161

Stern, S. A. & Levison, H. F. 2002, *Highlights Astron.*, 12, 205

Tancredi, G. & Favre, S. 2008 (*Paper I*) *Icarus*, 195, 851

Thirouin, A., Ortiz, J. L., Duffard, R., Santos-Sanz, P., Aceituno, F. J., & Morales, N. 2009, *A&A*, submitted